ACS SENSORS

pubs.acs.org/acssensors Article

Developing Fluorescence-Based Sensors to Support Rare Earth Element Separation

Poki Tse,* Alyssa F. Espley, Jason M. Rakos, Qingpu Wang, Chinmayee V. Subban, Samuel A. Bryan,* and Amanda M. Lines*

Cite This: https://doi.org/10.1021/acssensors.5c00833 Read Online

ACCESS | Metrics & More | Article Recommendations | Supporting Information

ABSTRACT: Rare earth elements (REEs) are essential to most renewable energy technologies. Unfortunately, as we transition to sustainable energy production, the demand for REEs rapidly grows well beyond the current rates of production. As a result, novel means of efficient, scalable, and easily adaptable methods for processing primary and recycled feedstocks are needed. Development and integration of sensors for highly selective in-line monitoring can support more efficient design and testing of such novel separation processes as well as more cost-effective deployment of those separation flowsheets. Work here will explore the application of fluorescence spectroscopy, a highly sensitive and selective technique, to quantify multiple lanthanides in complex mixtures, including known interferents or quenching agents. Results include identification of the optimal excitation wavelength and the limit of detection of various rare earth elements, as well as the performance of data-science-based quantification approaches in streams where "unknowns" are present. Overall, the data science tools in conjunction with optical sensor data were able to quantify analytes in the presence of other lanthanides anticipated to be in the actual industrial stream. Here, we include the characterization of lanthanides in a microfluidic device similar to those used in new process development. This study demonstrates the capability of utilizing fluorescence spectroscopy to quantify analytes in a complicated solution matrix, suggesting this as a successful approach for in-line monitoring to optimize the separation efficiency in an industrial stream.

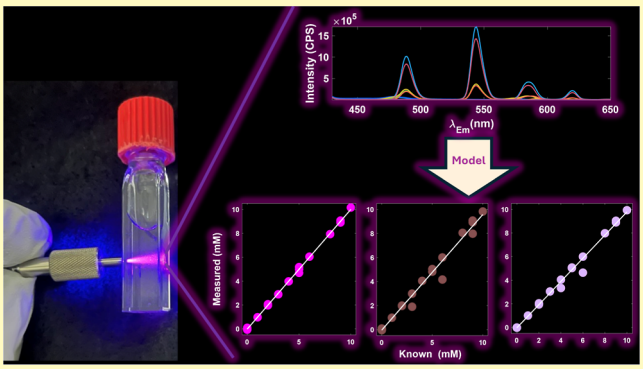

KEYWORDS: *online monitoring, fluorescence spectroscopy, lanthanides, chemometric analysis, rare earth elements*

The increase in global demand for rare earth elements (REEs) is due to their use in magnets needed for transportation, power generation, electric cars, and every-day electronics such as smartphones and speakers.[1−5] In particular, dysprosium (Dy), praseodymium (Pr), neodymium (Nd), samarium (Sm), yttrium (Y), and europium (Eu) are essential for production of the magnets.[2] Specifically, Nd and Dy are used for the fabrication of "permanent magnets" used in wind turbines and electric vehicles.[6,7] While the demand for REEs has grown exponentially, the production remains limited, with a few countries generating most of the global supply. To minimize any supply chain risks, there is a strong push to develop domestic REE production in the United States through a combination of primary (mines and natural brines) and secondary (recycled electronics) sources. Efforts to minimize the environmental impact of traditional mining approaches have led to exploration of alternative recovery methods.[8,9] However, considering the long-permitting and construction timelines for traditional mines, the recovery of REEs from nontraditional feed streams, such as recycling or industrial waste streams, which often have high concentrations of REEs, is gaining attention.[4,10−12]

Most feedstocks contain multiple REEs, and the extraction and purification of individual elements is challenging given that REEs exhibit very similar chemistries, due to similar ionic radii and oxidation states from the burial of f-orbital electrons within the electron orbitals.[3,13,14] The ability to obtain real-time chemical information for separation processes would allow rapid adaptability of novel separation methods to diverse feedstocks—accelerating domestic production of REEs. Most in-line sensors used in industrial-scale separations today are limited to the measurement of pH, temperature, salinity, etc., which do not offer any chemical information regarding the REEs. In-line monitoring with chemical information can

Received: March 12, 2025
Revised: April 5, 2025
Accepted: April 14, 2025

provide near real-time insight into solution conditions, which can be used to improve the separation process design and optimization.[15−17] Such insights into the in situ process chemistry would be immensely helpful for both more efficient REE separation process development and more cost-effective process deployment.

Optical spectroscopy-based sensors can provide in-depth information about chemical composition, oxidation state, and speciation.[18−20] Optical spectroscopy sensors are commonly used for in-line monitoring and provide nondestructive methods to quantify analytes under continuous operation.[21−24] Fluorescence spectroscopy offers particularly compelling benefits for the analysis of REEs because it is a sensitive and selective technique. Many REEs have unique fluorescence fingerprints produced selectively by exciting with specific wavelengths and can be characterized with relatively low limits of detection.[25] There is also excellent literature precedence for applying fluorescence spectroscopy to REE characterization where the fundamental analysis of luminescence properties of REEs is covered elsewhere.[25,26]

While extensive research and literature exists on the use of fluorescence-based quantification of REEs, their adoption and utilization in highly complex solutions as in-line sensors for accurate quantification are limited.[27,28] The first step toward the development of such sensors is advancing methods to accurately quantify REEs when interfering species are present (impacting sensor signal through various means), when single excitation wavelengths excite multiple REEs simultaneously (resulting in band overlap), or when challenging fluorescence backgrounds are present from the reaction vessels or process matrices. Utilizing chemical data science approaches can help overcome these challenges and expand the applicability and utility of fluorescence-based sensors. Chemometric analysis is an example of one potential tool, which is a mathematical and statistical approach to finding the relationship between the spectral changes and analyte properties.[29−31] Utility of these approaches is explored here, along with identification of a wide range of potential spectral complexities that must be characterized to support application of fluorescence sensors to REE separations. The authors have developed a laminar coflow method to selectively precipitate Dy from a mixed Nd and Dy aqueous solution in a microfluidic device based on a flow-induced nonequilibrium condition, and it has been covered in another manuscript.[1] This work focuses on utilizing fluorescence spectroscopy to characterize solutions containing several lanthanides in an aqueous solution including Eu, Dy, Pr, Tb, and Nd in both a cuvette and a microfluidic device to prepare for efforts to apply sensors to REE separation processes. The characterization of solid lanthanides will be covered in future work. While our interest in the recycling of these specific lanthanides is related to their utility as critical materials for advanced technology needs, this sensor system can be applied to essentially all lanthanides based on their fluorescence properties.[32−36]

EXPERIMENTAL SECTION

Chemicals. Neodymium ($NdCl_3{\cdot}6\ H_2O$, 99.9%), dysprosium ($DyCl_3{\cdot}6\ H_2O$, 99.9%), yttrium ($YCl_3{\cdot}6\ H_2O$, 99.9%), europium ($EuCl_3{\cdot}6\ H_2O$, 99.9%), praseodymium ($PrCl_3{\cdot}H_2O$, 99.9%), and terbium ($TbCl_3{\cdot}6\ H_2O$, 99.9%) hydrated chloride salts were sourced from Sigma-Aldrich. Cobalt ($Co(NO_3)_2{\cdot}6\ H_2O$, 99%) and nickel ($Ni(NO_3)_2{\cdot}6\ H_2O$, 98%) hydrated nitrate salts were sourced from Thermo Fisher Scientific. Scandium nitrate (99.9%) was sourced from Research Chemicals. All solutions were prepared by dissolving an appropriate amount of chemical in ≥ 18.2 M Ω·cm deionized water.

Equipment. A Fluoromax Plus C fluorimeter equipped with a 150 W xenon lamp and an R928P photon counting photomultiplier tube was utilized for the fluorescence measurements. A 1 × 1 cm cuvette holder stage was utilized to maintain a consistent light path throughout the experiments. The instrument was assessed daily to measure any drift in the wavelength or signal intensity using a reference provided by the quinine sulfate fluorescence intensity reference. FluorEssence software was used to control the instrument integration time, slit widths, execution wavelengths, and emission wavelengths. The integration time is 0.5 s. Triplicate scans were collected for each sample, and these spectra were averaged to 1 spectrum per sample for analysis. The data was imported into Origin for data extraction. The data was subsequently analyzed, and plots were generated using MATLAB (version R2023b, Mathworks, Natick, MA).

Chemometric Analysis. All chemometric models were generated using the eigenvector Research PLS Toolbox (version 9.3.1, eigenvector Research, Inc., Manson, WA). The training set contained different concentrations of Eu, Dy, and Tb, as shown in Table S1. The preprocessing methods employed on the training set included the first derivative and mean centering. The first derivative can emphasize the area of spectral changes, and mean centering can avoid the bias created by samples with higher analyte concentration.[30,37] Mean centering was also applied to the concentration matrix. Three partial least-squares (PLS) models were built for each analyte excitation wavelength (350 nm for Dy, 368 nm for Tb, and 393 nm for Eu). The PLS analysis relates and captures the main variances between spectroscopic and concentration data into new abstract latent variable (LV) factors.[17] There were two validation sets where the first set contained only the analytes present in the training set, and the second set included Nd, which the model had not encountered before. This was used to test the ability of the model to quantify analytes in the presence of unanticipated interferents.

The model performance can be evaluated based on statistics associated with the model results including the regression coefficient (R^2), which relates to the fit of prediction, the root-mean-square error of calibration (RMSEC), the root-mean-square error of cross validation (RMSECV), and the root-mean-square error of prediction (RMSEP). RMSEC evaluates the model performance by using the entire training set. RMSECV evaluates the model performance by selectively removing a group of data and using the remaining samples to build a model to predict analyte concentration of those excluded samples. This cross-validation method provides a good estimate of the model performance on the unknown data set. The cross-validation method applied in this manuscript was the venetian blind method with 5 splits and a blind thickness of 1. RMSEP is a more challenging model evaluation approach since the model is applied to the data set that has not been used for model development.[16,30,37]

Measurements in a Microfluidic Device. Fluorescence measurements were also performed in a microfluidic device designed and used in previous work for REE separations.[1] The device consisted of a cut parafilm membrane sandwiched between two microscope glass slides, as shown in Figure 1. The glass material was used to minimize the fluorescence interference from plastic materials such as polycarbonate in this design. Three holes were drilled onto the top plate as the inlets and outlet, where barb fittings were glued using an epoxy glue. A Y-shaped pattern was cut on the parafilm membrane as the fluidic channel using a cutter (Silhouette Portrait 3). The straight part of the Y channel measured 0.5 × 3 × 35 mm^3. The three layers were aligned, fastened with binder clips, and heated on a hot plate at 125 °C for 2 min. After cooling, the melted parafilm resolidified and sealed the two glass slides securely. The MFD was then placed in a fluorometer for measurement. During the measurement, two syringes containing mixed rare earth chloride solutions were simultaneously injected into the microfluidic device at a constant flow rate of 1 mL/min using a programmable syringe pump (NE-4000, New Era Pump Systems Inc.).

https://doi.org/10.1021/acssensors.5c00833
ACS Sens. XXXX, XXX, XXX−XXX

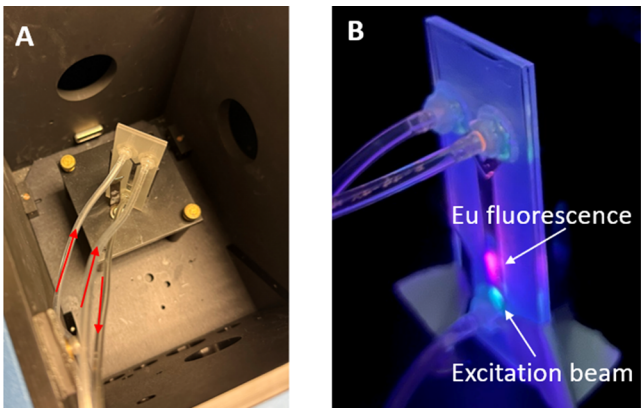

Figure 1. Experimental setup of the coflow experiment. (A) Setup of the MFD inside the spectrofluorometer. (B) MFD under the fluorescence measurement of an Eu solution.

RESULTS AND DISCUSSION

Rare Earth Element Characterization. Fluorescence spectroscopy is a highly sensitive and selective optical technique that can perform both quantitative and qualitative analysis of REEs including Dy, Eu, and Pr. The variation of excitation wavelength can result in different emission intensities and even profiles of analytes, as shown in Figure 2. Therefore, it is important to find the optimum excitation wavelength that maximizes the analytical signal while minimizing potential background signals. For an initial exploration, optimum excitation wavelength, corresponding emission peak, and limit of detection (LOD) of each analyte were determined in pure component systems and is covered in Table 1. These data lay the benchmark of the optimal performance and provide the necessary insight for selecting target excitation wavelengths after knowledge is gained on background interferences. Note that when optimizing spectral collection parameters for different reaction vessels or process streams, it may be necessary to choose an excitation wavelength that is shifted slightly from the optimal excitation wavelength. This can allow for balance between optimizing the target signal and minimizing background signals. While this was not required in the work discussed here, modifications for future applications may need to be explored.

Table 1. Limit of Detection (LOD) of Different Single-Component Samples of REEs Measured in the 1 cm Cuvette, Utilizing the Excitation Wavelength Identified to Output the Highest Intensity Emission

analyte	excitation wavelength (nm)	emission wavelength (nm)	measured LOD in 1 cm cuvette
Dy	350	479	0.192 mM [72.4 ppm]
	350	574	0.227 mM [85.6 ppm]
Eu	393	592	0.00334 mM [1.2 ppm]
Pr	255	357	0.00174 mM [0.4 ppm]

The sensitivity of sensor measurement can be estimated by determining the lower limit of detection (LOD), as calculated using the equation shown below.[38] Calibration plots used to provide values for calculations can be seen in Figures 3 and S1

$$\mathrm{LOD} = \frac{3s}{m}$$

where s is the standard deviation of a blank, and m is the slope of the calibration curve. The calculated limits of detection are not necessarily optimized here (via instrument settings), but even this initial pass shows a limit of detection that could support analysis in a range of potential streams for harvesting REEs, including some industrial streams, which is around hundreds of ppm.[39−41] Optimization or reduction of LODs can potentially be achieved but will be the focus of future work.

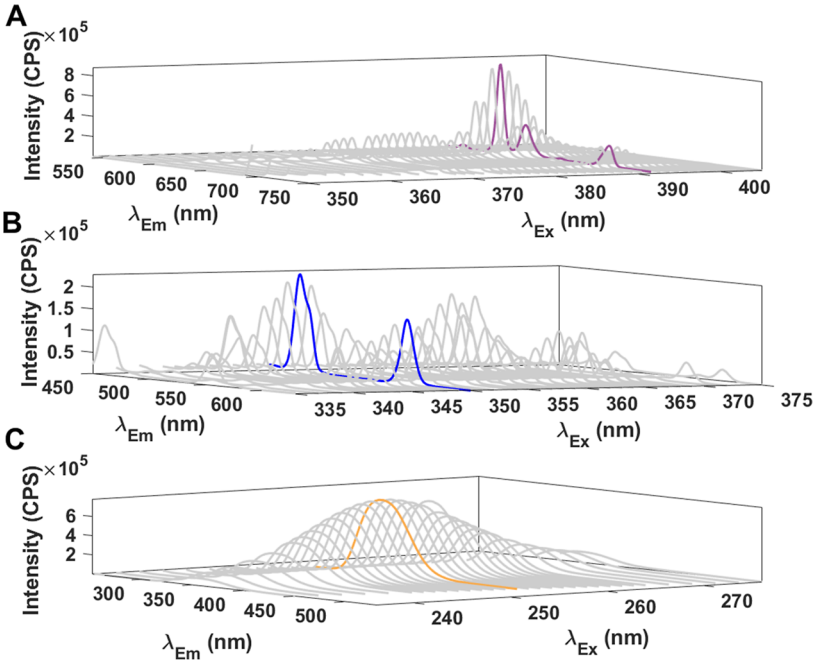

Figure 2. Fluorescence spectra of (A) Eu, (B) Dy, and (C) Pr scanned at various excitation wavelengths. The colored line was the emission spectra collected at optimum excitation wavelength, as shown in Table 1

https://doi.org/10.1021/acssensors.5c00833
ACS Sens. XXXX, XXX, XXX−XXX

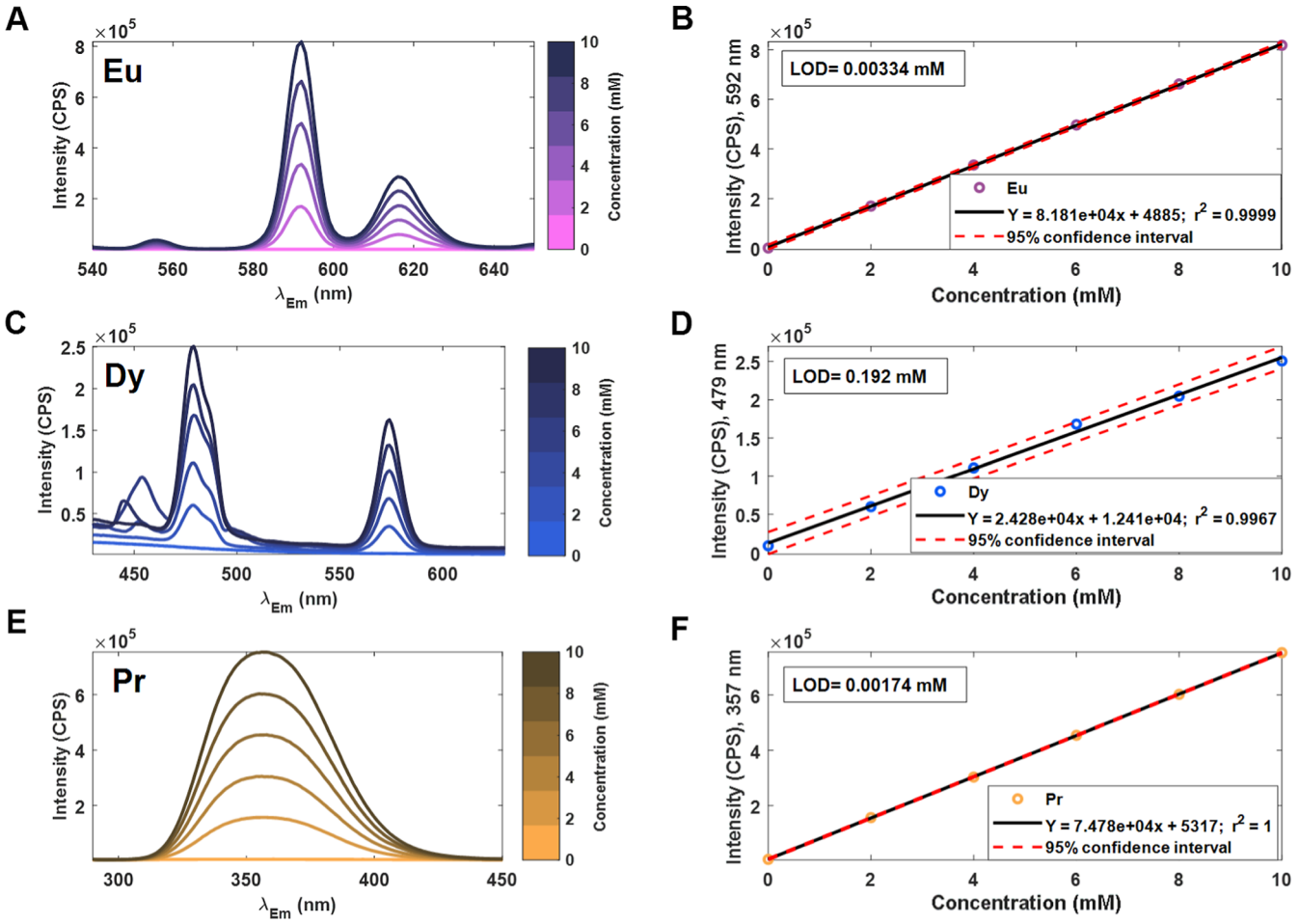

Figure 3. Emission spectra at different concentrations for (A) Eu, (C) Dy, and (E) Pr along with the corresponding calibration curves for the (B) Eu emission peak at 592 nm, (D) Dy emission peak at 479 nm, and (F) Pr emission peak at 357 nm. The calibration curve of Dy emission peak at 574 nm is shown in Figure S1.

Interference Effect. A major challenge of developing and monitoring novel separation schemes of REEs from nontraditional feeds is the presence of large amounts of interferents. Key examples, especially from some industrial streams, include Co, Ni, Sc, and Y. Co and Ni can be found in the NdFeB permanent magnet,[42] and they are also considered critical materials.[43] Sc and Y can be found in acid mine drainage.[44] These interferents can impact process chemistry and performance but also impact the optical monitoring of the REEs in the process line. Therefore, understanding the interference effects on REE spectral signatures is essential. This work studied the effect of some common interferents (Co, Ni, Sc, and Y) on solutions of 10 mM of Eu, Dy, and Pr, respectively, as shown in Figure 4.

All interferents affect the spectral signature of Eu, Dy, and Pr, and each interferent has a different effect on the analyte emission peaks, as shown in Figure 4. Both quenching and sensitizing effects on analyte emission intensity were observed among these interferents. For example, the presence of Co, Ni, and Sc reduced the emission intensity of Pr. The presence of interferents can pose a variety of challenges to the accurate quantification of analytes. This work will begin to explore two example cases of this: band overlap from coexcited analytical targets and quenching effects from interferents. Ultimately, data science tools will need to be expanded to account for the presence of interferences expected in different process feed streams, which will be the focus of the future work. The next section demonstrates how chemometric models can account for overlapping bands and quenching effects and accurately quantify analytes in complex solution matrix. Generally, the combination of data science tools with the fluorescence approach can enable more broadly applicable sensor design and operation.

Analyte Quantification in Complicated Solution Matrix. It is essential to quantify multiple analytes simultaneously in an industrial stream to optimize the separation efficiency and keep researchers and operators informed of the process conditions. As demonstrated above, advanced means of data analysis are required to support accurate quantification of REEs. Here, the use of chemometric modeling is discussed in regard to the quantification of Dy, Tb, and Eu in a mixed aqueous lanthanide sample prepared in the laboratory, with results shown in Figure 5. The wavelengths used to excite Dy, Tb, and Eu are 350, 368, and 393 nm, respectively, and all samples were scanned at these three excitation wavelengths. Note that in an industrial setting, this can be done one of two ways: (1) using a multiplexor to switch between excitation sources and (2) using a combined excitation source. For each method, trade-offs exist in response time vs complexity of data analysis, and an in-depth exploration of this will be the focus of future work. Here, the effects of switching between light sources are explored, particularly looking to observe impacts on accuracy

https://doi.org/10.1021/acssensors.5c00833
ACS Sens. XXXX, XXX, XXX−XXX

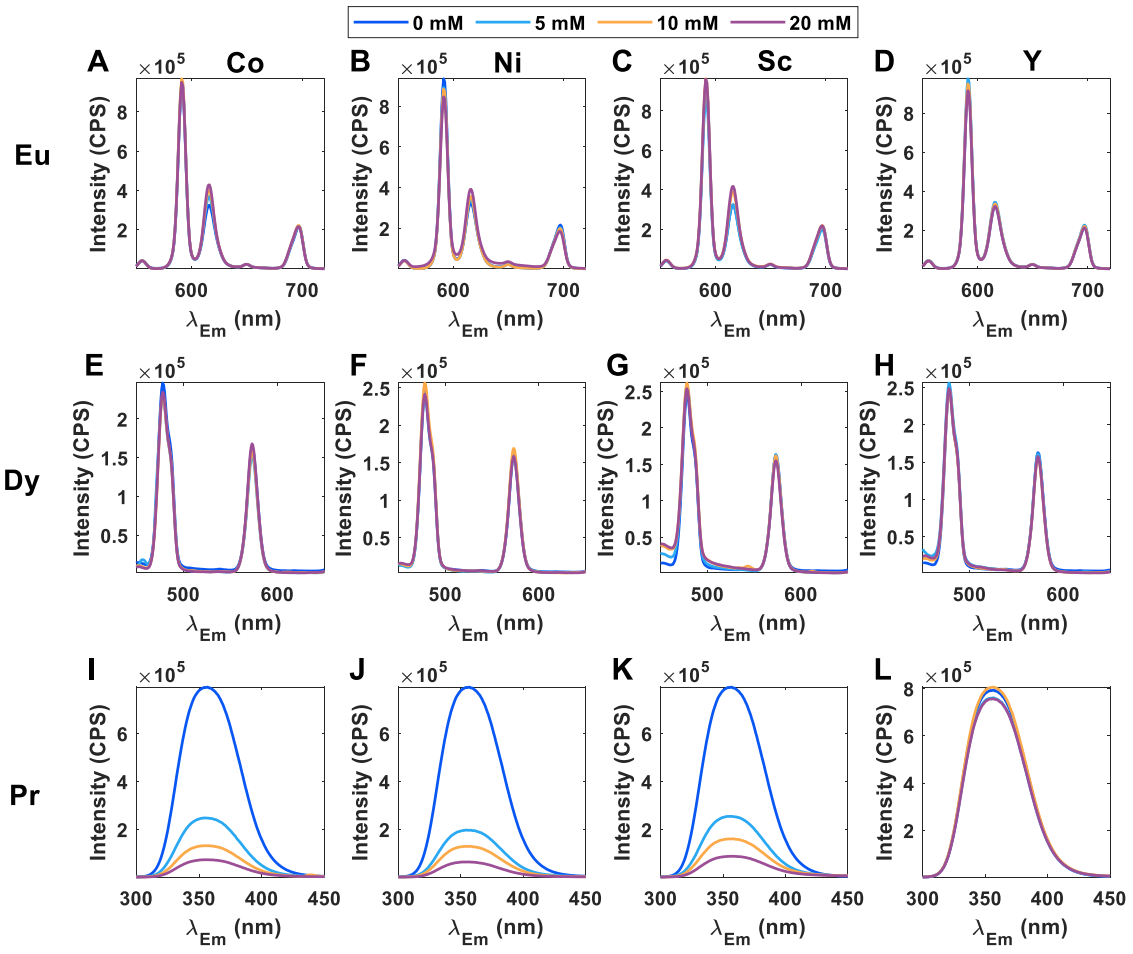

Figure 4. Interference effects on the emission peaks of Eu, Dy, and Pr. Eu spectra with various concentrations of interferents shown for (A) Co, (B) Ni, (C) Sc, and (D) Y. Dy spectra with various concentrations of interferents are shown for (E) Co, (F) Ni, (G) Sc, and (H) Y. Pr spectra with various concentrations of interferents shown for (I) Co, (J) Ni, (K) Sc, and (L) Y.

in the cases where interferents are present. This includes REE mixtures where a single excitation source wavelength will elicit emissions from more than one REE present, resulting in band overlap as well as the quenching effects observed inside mixtures. Figure 5 provides examples of the complex spectra produced from the optical interrogation of a series of multicomponent mixtures. These spectra were from a consistent sample set when varying the excitation wavelength from 350 nm (ideal excitation for Dy) in Figure 5A to 368 nm (ideal excitation for Tb) in Figure 5B and to 393 nm (ideal excitation for Eu) for Figure 5C. Figure 5C provides a strong example for the selectivity of fluorescence spectroscopy, where, from a qualitative standpoint, the clean Eu fingerprint appears visible even in mixed samples. However, it is key to contrast this with Figure 5A, which provides a powerful example of the potential complexity of spectra. In this case, the excitation wavelength for Dy was used, but it will catch the tail end of the excitation profile for Tb. This leads to the ingrowth of Tb bands overlapping Dy bands around 480 nm, which directly interfere with Dy bands, so Dy and Tb were included in the training set to explore how the band overlap affects the accuracy of analyte quantification.

To explore how spectral complexity could impact the accuracy of quantification, three PLS models were developed to quantify Dy, Eu, and Tb concentrations based on their excitation wavelength. The model results are shown in Figure 6 and Table 2. As noted in the experimental section and Table S1, Nd was included in three validation samples to test the model robustness in the face of unanticipated conditions. Despite the complexity of the spectra observed in Figure 5A, the concentration of Dy was accurately measured even in the presence of Tb. In addition, the presence of Nd did not appear to affect the Dy model performance. Furthermore, RMSEC and RMSECV values are similar, indicating an overall robust model. This demonstrated chemometric analysis partnered with the fluorescence-based sensor can accurately quantify analytes in the presence of other directly interfering analytes.

The performances of the Tb and Eu models are more complex, which is interesting given the apparent relative simplicity of the spectral plots. The model-measured concentrations of Tb and Eu were similar to the known concentrations for the training set samples and the validation samples without Nd, as shown in Figure 6B,C. Results for the Nd-containing samples (red line in Figure 5) were slightly lower than the known concentration, which ultimately increased the prediction error (RMSEP). The lower measured concentration in those Nd-containing samples might be due to the quenching of Nd on Eu and Tb fluorescence via nonradiative energy transfer, which results in Eu and Tb having higher RMSEPs than Dy.[45,46] Future work will be done to include Nd-containing samples in the training set so the model can study the effect of Nd quenching on Tb and Eu

https://doi.org/10.1021/acssensors.5c00833
ACS Sens. XXXX, XXX, XXX−XXX

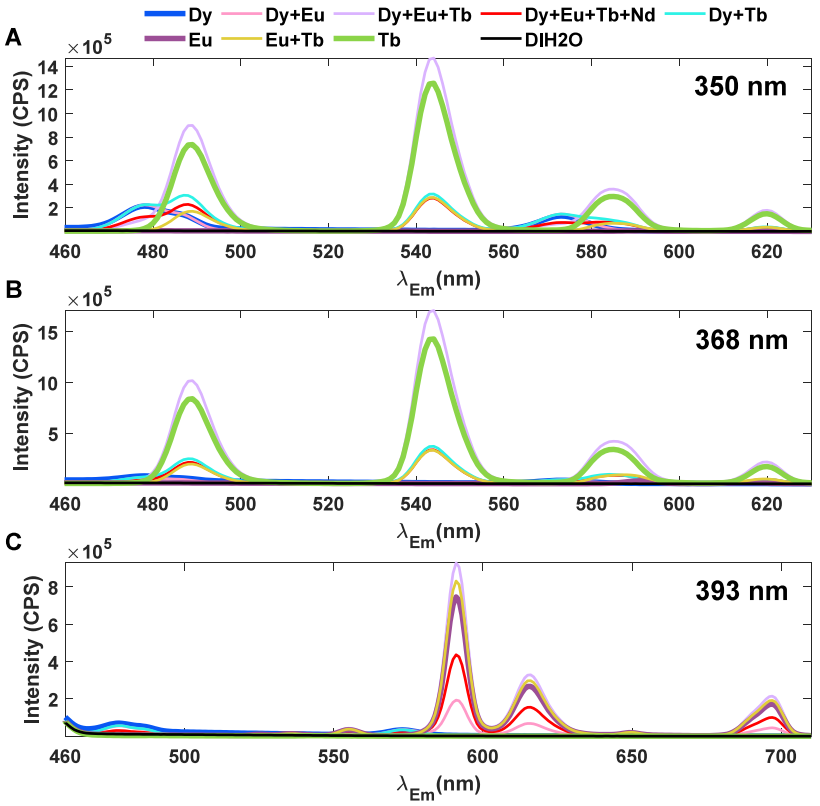

Figure 5. Emission spectrum of a series of single and multicomponent samples excited at (A) 350 nm, (B) 368 nm, and (C) 393 nm. The composition of each sample was Dy: 8 mM Dy; Dy + Eu: 9 mM Dy and 2 mM Eu; Dy + Eu + Tb: 3 mM Dy, 10 mM Eu, and 10 mM Tb; Dy + Eu + Tb + Nd: 5 mM Dy, 6 mM Eu, 3 mM Tb, and 10 mM Nd; Dy + Tb: 9 mM Dy and 2 mM Tb; Eu: 8 mM Eu; Eu + Tb: 9 mM Eu and 2 mM Tb; and Tb: 8 mM Tb.

Table 2. Statistics of Three PLS Models

model	excitation wavelength (nm)	analyte	RMSEC	RMSECV	RMSEP
1 (2LV)	350	Dy	0.06	0.08	0.2
2 (3LV)	368	Tb	0.06	0.08	1
3 (2LV)	393	Eu	0.04	0.05	0.6

spectra. In addition, the lanthanide quenching discussion and its effect on lanthanide quantification will be further examined in future work. Overall, the models performed well on most spectral complexities, producing accurate quantification tools. Further work is needed to explore robust means of quantification in the presence of quenching agents.

Monitoring Rare Earth Elements in a Microfluidic Device. Development of novel separation schemes, especially those using costly separation targets, can be more economically and efficiently completed at the microscale. To support work at this small scale, the application of these techniques in microfluidic devices (MFDs) was explored for organic solvent extraction[47,48] and precipitation-based separation in aqueous solutions.[1] Ideal REE separation processes allow high selectivity even when REEs are in low concentrations, operate continuously for large-volume mineral recovery, and rely on sustainable chemicals and solvents. To simulate such relevant mineral extraction conditions at the small scale, an MFD was used that allows flow-based selective REE precipitation in aqueous media. The MFD was adapted to fit inside a spectrofluorometer to allow the interface to be measured, as shown in Figure 1. While this is not a setup that would be used for in-line analysis of commercial processes, it provides a valuable benchmark for these applications. Development and utilization of more flexible and robust systems for in-line measurement will be the focus of future work.

Multicomponent samples were premixed at various Eu and Dy concentrations and were injected into an MFD, which was excited at ideal wavelengths for both Eu and Dy (see Table 1or 2 for values) where resulting spectra are shown in Figure 7. Here, concentrations of REE introduced to the MFD were higher than those measured in a cuvette to compensate for the fact that the fluorimeter excitation and collection optics were not readily optimizable to account for MFD geometry. The high fluorescence baseline is due to the fluorescence of the MFD material and provides a useful example of additional interfering signals that must be accounted for in effective quantification approaches. No Dy emission peak was observed when the multicomponent samples were excited at the Eu excitation wavelength (393 nm), but the presence of Dy enhanced the Eu fluorescence intensity when the Dy concentration was greater than 1 M, as shown in Figures 7 and S2. Similar observations were obtained when the multicomponent samples were excited at the Dy excitation wavelength (350 nm), and the presence of Eu enhanced the Dy fluorescence intensity when Eu concentration was greater than 1 M. Overall, this demonstrated the fluorescence sensor can be applied to multiple experimental configurations and provides the needed proof of principle that this approach is applicable to in-line monitoring of REE separation at the microfluidic scale. It also reinforces the range of potential complexities that can be anticipated from optical sensor

https://doi.org/10.1021/acssensors.5c00833
ACS Sens. XXXX, XXX, XXX−XXX

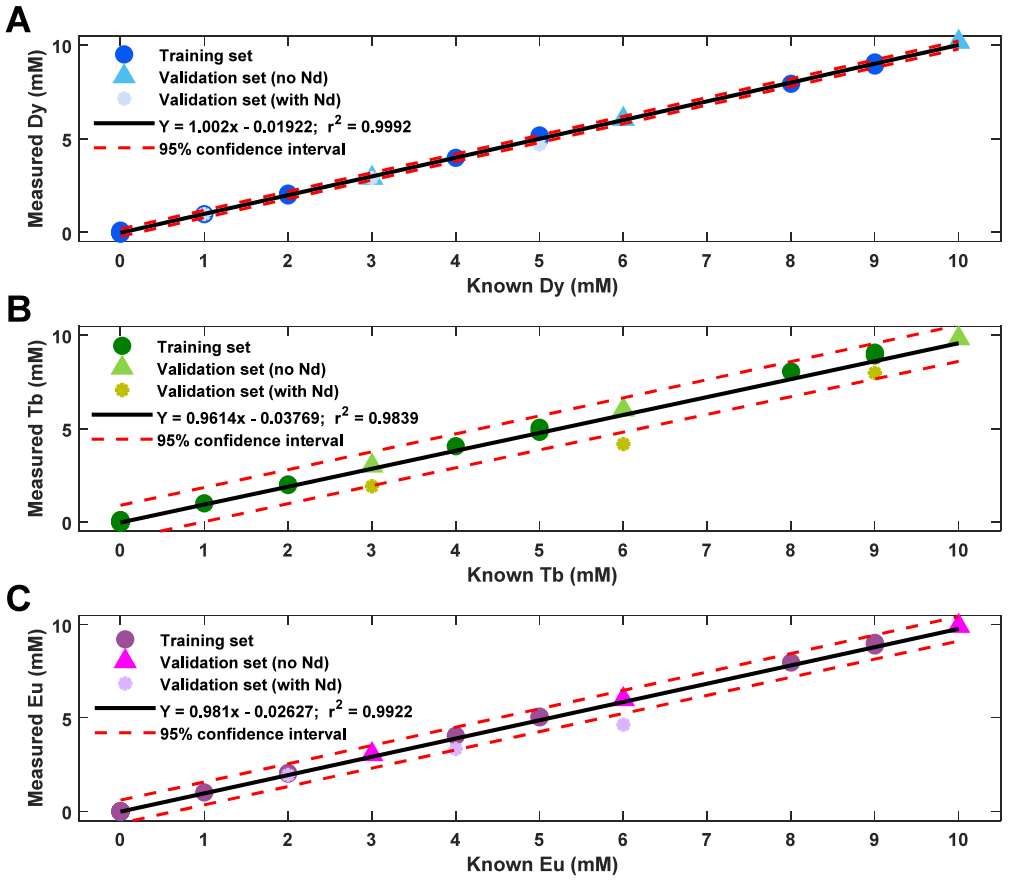

Figure 6. Comparison between known (A) Dy, (B) Tb, and (C) Eu concentrations and model-measured concentrations.

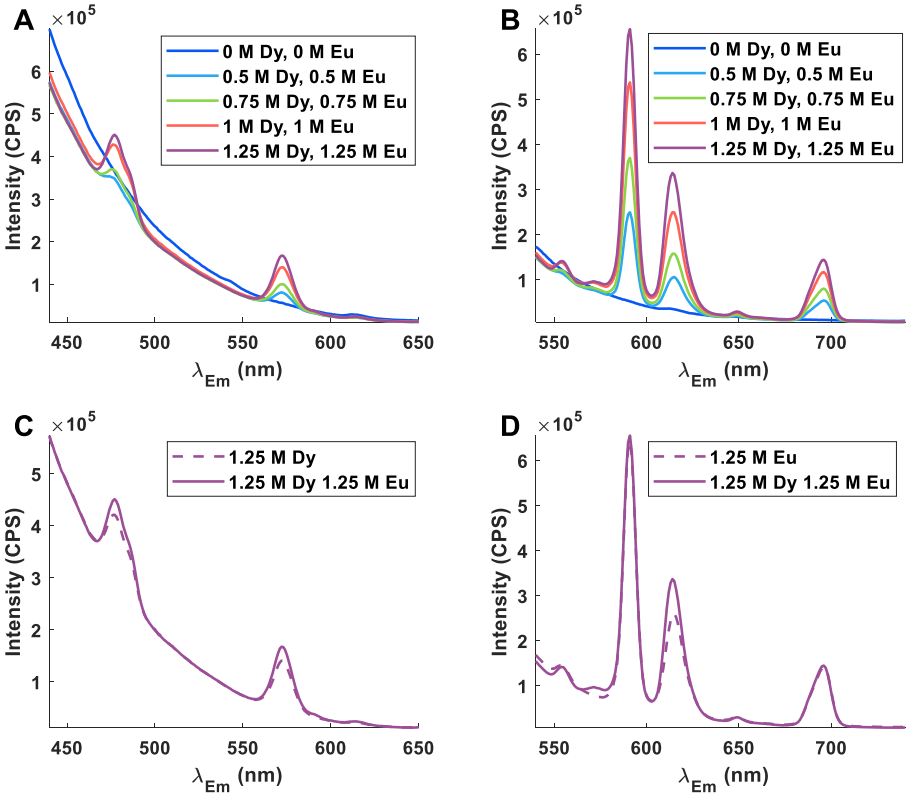

Figure 7. On-chip fluorescence sensor spectra collected for multicomponent samples excited at (A) 350 nm and (B) 393 nm. The comparison between pure and multicomponent spectra at (C) 350 nm and (D) 393 nm.

https://doi.org/10.1021/acssensors.5c00833
ACS Sens. XXXX, XXX, XXX−XXX

interrogation of these REE-containing systems and reinforces the need for advanced data analysis approaches. The future work will focus on developing real-time analyte quantification in MFDs.

CONCLUSIONS

The market demand for REE materials is increasing rapidly, and concerns exist about harvesting enough material to meet demands from traditional mining operations. Harvesting REEs from nontraditional sources could be a game-changing option, but new separation processes need to be developed. The best route for timely process development and cost-effective deployment relies on the effective use of sensors for in-line monitoring. Optical based sensors provide a robust and unique option for in-depth chemical composition analysis, but signals can be highly complex. This work explored the optical fingerprint and potential signal interferences for selected REEs including Dy, Pr, Eu, and Tb via fluorescence spectroscopy. This includes identification of optimal excitation wavelengths, signal impacts of transition metal interferents, band overlap, nonselectivity of excitation wavelengths, quenching effects, and fluorescence background from reaction vessels (i.e., a microfluidic device). Overall, work indicates that fluorescence spectroscopy can be a highly selective sensor for REE characterization and quantification in complex solutions but that advanced data analysis approaches must be included in the sensor package to overcome optical complexities. Here, chemometric modeling, a form of chemical data science, was used to quantify multiple REEs in multicomponent samples with high levels of accuracy. This lays the foundation for the further advancement of fluorescence-based sensors partnered with data science to provide the in-line and real-time characterization of novel REE separation processes.

ASSOCIATED CONTENT

Supporting Information

The Supporting Information is available free of charge at https://pubs.acs.org/doi/10.1021/acssensors.5c00833.

Composition of training and validation data sets; calibration curve for Dy showing the fluorescence emission intensity at 574 nm vs concentration; and comparison plot of emission spectra between pure and premixed Dy and Eu (PDF)

AUTHOR INFORMATION

Corresponding Authors

Poki Tse − *Pacific Northwest National Laboratory, Richland, Washington 99352, United States;* orcid.org/0000-0003-2901-9509; Email: poki.tse@pnnl.gov

Samuel A. Bryan − *Pacific Northwest National Laboratory, Richland, Washington 99352, United States;* orcid.org/0000-0002-8826-0880; Email: sam.bryan@pnnl.gov

Amanda M. Lines − *Pacific Northwest National Laboratory, Richland, Washington 99352, United States;* Email: amanda.lines@pnnl.gov

Authors

Alyssa F. Espley − *Pacific Northwest National Laboratory, Richland, Washington 99352, United States*

Jason M. Rakos − *Pacific Northwest National Laboratory, Richland, Washington 99352, United States*

Qingpu Wang − *Pacific Northwest National Laboratory, Richland, Washington 99352, United States;* orcid.org/0000-0001-5604-1571

Chinmayee V. Subban − *Pacific Northwest National Laboratory, Richland, Washington 99352, United States; Department of Materials Science and Engineering, University of Washington, Seattle, Washington 98195, United States;* orcid.org/0000-0002-0100-4121

Complete contact information is available at: https://pubs.acs.org/10.1021/acssensors.5c00833

Notes

The authors declare no competing financial interest.

ACKNOWLEDGMENTS

The authors thank Dr. Heather M. Felmy for technical support. This work was supported by the Laboratory Directed Research and Development (LDRD) program at PNNL, under the Non-Equilibrium Transport Driven Separations (NETS) Initiative. PNNL is a multiprogram national laboratory operated for the U.S. Department of Energy (DOE) by Battelle Memorial Institute under Contract No. DE-AC05-76RLO 1830.

REFERENCES

(1) Wang, Q.; Subban, C. V. Flow-driven enhancement of neodymium and dysprosium separation from aqueous solutions. *RSC Sustainability* **2024**, *2* (5), 1400−1407.

(2) Barros, O.; Costa, L.; Costa, F.; Lago, A.; Rocha, V.; Vipotnik, Z.; Silva, B.; Tavares, T. Recovery of Rare Earth Elements from Wastewater Towards a Circular Economy. *Molecules* **2019**, *24* (6), 1005.

(3) DOE. *Rare Earth Recycling*. 2020. https://science.osti.gov/bes/Highlights/2017/BES-2017-03-c accessed.

(4) Dodson, J. R.; Hunt, A. J.; Parker, H. L.; Yang, Y.; Clark, J. H. Elemental sustainability: Towards the total recovery of scarce metals. *Chem. Eng. Process.* **2012**, *51*, 69−78.

(5) Adeel, M.; Lee, J. Y.; Zain, M.; Rizwan, M.; Nawab, A.; Ahmad, M. A.; Shafiq, M.; Yi, H.; Jilani, G.; Javed, R.; et al. Cryptic footprints of rare earth elements on natural resources and living organisms. *Environ. Int.* **2019**, *127*, 785−800.

(6) Golroudbary, S. R.; Makarava, I.; Kraslawski, A.; Repo, E. Global environmental cost of using rare earth elements in green energy technologies. *Sci. Total Environ.* **2022**, *832*, 155022.

(7) Fishman, T.; Graedel, T. E. Impact of the establishment of US offshore wind power on neodymium flows. *Nat Sustainability* **2019**, *2* (4), 332−338.

(8) Maani, T.; Mathur, N.; Singh, S.; Rong, C.; Sutherland, J. W. Potential for Nd and Dy Recovery from End-of-Life Products to Meet Future Electric Vehicle Demand in the U.S. *Procedia CIRP* **2021**, *98*, 109−114.

(9) Xie, F.; Zhang, T. A.; Dreisinger, D.; Doyle, F. A critical review on solvent extraction of rare earths from aqueous solutions. *Miner. Eng.* **2014**, *56*, 10−28.

(10) Conrad, R.. *Rare Earth Elements* 2023.

(11) Yang, Y.; Walton, A.; Sheridan, R.; Güth, K.; Gauß, R.; Gutfleisch, O.; Buchert, M.; Steenari, B.-M.; Van Gerven, T.; Jones, P. T.; et al. REE Recovery from End-of-Life NdFeB Permanent Magnet Scrap: A Critical Review. *J. Sustain. Metall.* **2017**, *3* (1), 122−149.

(12) Costis, S.; Mueller, K. K.; Coudert, L.; Neculita, C. M.; Reynier, N.; Blais, J.-F. Recovery potential of rare earth elements from mining and industrial residues: A review and cases studies. *J. Geochem. Explor.* **2021**, *221*, 106699.

(13) Opare, E. O.; Struhs, E.; Mirkouei, A. A comparative state-of-technology review and future directions for rare earth element separation. *Renew. Sustain. Energy Rev.* **2021**, *143*, 110917.

(14) Tse, P.; Bessen, N. P.; Galley, S. S.; Bryan, S. A.; Lines, A. M.; Shafer, J. Electrochemical Oxidation and Speciation of Lanthanides in Potassium Carbonate Solution. *J. Electrochem. Soc.* **2022**, *169* (4), 046521.
(15) Tse, P.; Bryan, S. A.; Bessen, N. P.; Lines, A. M.; Shafer, J. C. Review of On-line and Near Real-time Spectroscopic Monitoring of Processes Relevant to Nuclear Material Management. *Anal. Chim. Acta* **2020**, *1107*, 1−13.
(16) Tse, P.; Shafer, J.; Bryan, S. A.; Lines, A. M. Quantification of Raman-Interfering Polyoxoanions for Process Analysis: Comparison of Different Chemometric Models and a Demonstration on Real Hanford Waste. *Environ. Sci. Technol.* **2021**, *55* (19), 12943−12950.
(17) Tse, P.; Shafer, J.; Bryan, S. A.; Nelson, G. L.; Lines, A. M.; Measuring, Nd Measuring Nd(III) Solution Concentration in the Presence of Interfering Er(III) and Cu(II) Ions: A Partial Least Squares Analysis of Ultraviolet−Visible Spectra. *Appl. Spectrosc.* **2021**, *76* (2), 173−183.
(18) Boily, N. T. C.; Felmy, H. M.; Medina, A. S.; Bello, J. M.; Bryan, S. A.; Lines, A. M. Development of an Attenuated Total Reflectance−Ultraviolet−Visible Probe for the Online Monitoring of Dark Solutions. *ACS Sensors* **2025**, *10* (1), 122−132.
(19) Cui, X.; Wang, H.; Wang, X.; Tang, Y.; Zhang, Y.; Dong, Y.; Jing, L.; Shen, L. Room Temperature and Humidity Resistant NH3 Detection Based on a Composite of Hydrophobic CNTs with Sulfur Nanosheets. *ACS Sensors* **2025**, *10*, 1756.
(20) Morse, J.; Ofodum, N.; Tang, F. K.; Schmidt, M.; Lu, X.; Leung, K. Leveraging Metal Complexes for Microsecond Lifetime-Based Chloride Sensing. *ACS Sensors* **2025**, *10* (2), 657−663.
(21) Bryan, S. A.; Levitskaia, T. G.; Casella, A. J.; Peterson, J. M.; Johnsen, A. M.; Lines, A. M.; Thomas, E. M.. In *Chapter 4 - Spectroscopic On-Line Monitoring for Process Control and Safeguarding of Radiochemical Streams in Nuclear Fuel Reprocessing Facilities. In Advanced Separation Techniques for Nuclear Fuel Reprocessing and Radioactive Waste Treatment*; Nash, K. L., Lumetta, G. J., Eds.; Woodhead Publishing, 2011; pp 95−119.
(22) Lines, A. M.; Nelson, G. L.; Casella, A. J.; Bello, J. M.; Clark, S. B.; Bryan, S. A. Multivariate Analysis To Quantify Species in the Presence of Direct Interferents: Micro-Raman Analysis of HNO3 in Microfluidic Devices. *Anal. Chem.* **2018**, *90* (4), 2548−2554.
(23) Casella, A. J.; Ahlers, L. R. H.; Campbell, E. L.; Levitskaia, T. G.; Peterson, J. M.; Smith, F. N.; Bryan, S. A. Development of Online Spectroscopic pH Monitoring for Nuclear Fuel Reprocessing Plants: Weak Acid Schemes. *Anal. Chem.* **2015**, *87* (10), 5139−5147.
(24) Casella, A.; Lines, A.; Nelson, G.; Bello, J.; Bryan, S. MicroRaman Measurements for Nuclear Fuel Reprocessing Applications. *Procedia Chem* **2016**, *21*, 466−472.
(25) Introduction to Fluorescence. *Principles of Fluorescence Spectroscopy*, 3rd ed.; Lakowicz, J. R., Ed.; Springer, 2006.
(26) Binnemans, K. Interpretation of europium(III) spectra. *Coord. Chem. Rev.* **2015**, *295*, 1−45.
(27) Liu, W.; Huang, Y.; Ji, C.; Grimes, C. A.; Liang, Z.; Hu, H.; Kang, Q.; Yan, H.-l.; Cai, Q.-Y.; Zhou, Y.-G. Eu3+-Doped Anionic Zinc-Based Organic Framework Ratio Fluorescence Sensing Platform: Supersensitive Visual Identification of Prescription Drugs. *ACS Sensors* **2024**, *9* (2), 759−769.
(28) Huang, P.-J. J.; Vazin, M.; Lin, J. J.; Pautler, R.; Liu, J. Distinction of Individual Lanthanide Ions with a DNAzyme Beacon Array. *ACS Sensors* **2016**, *1* (6), 732−738.
(29) Tse, P.; Bessen, N. P.; Hall, G. B.; Seiner, B. N.; Lumetta, G. J.; Bryan, S. A.; Lines, A. M. A Review of Online Monitoring within Used Nuclear Fuel Recycling Processes. *Solvent Extr. Ion Exch.* **2024**, *42* (5), 347−380.
(30) Otto, M. *Chemometrics: Statistics and Computer Application in Aanalytical Chemistry*; John Wiley & Sons Inc., 2017.
(31) Lackey, H. E.; Sell, R. L.; Nelson, G. L.; Bryan, T. A.; Lines, A. M.; Bryan, S. A. Practical Guide to Chemometric Analysis of Optical Spectroscopic Data. *J. Chem. Educ.* **2023**, *100* (7), 2608−2626.
(32) Fuchs, M. C.; Beyer, J.; Lorenz, S.; Sharma, S.; Renno, A. D.; Heitmann, J.; Gloaguen, R. A spectral library for laser-induced fluorescence analysis as a tool for rare earth element identification. *Earth Syst. Sci. Data* **2021**, *13* (9), 4465−4483.
(33) Zhao, Q.; Liu, X.-M.; Li, H.-R.; Zhang, Y.-H.; Bu, X.-H. High-performance fluorescence sensing of lanthanum ions (La3+) by a polydentate pyridyl-based quinoxaline derivative. *Dalton T* **2016**, *45* (26), 10836−10841.
(34) Hagan, J. J.; Taylor, S. C.; Tweedle, M. F. Fluorescence detection of gadolinium chelates separated by reversed-phase high-performance liquid chromatography. *Anal. Chem.* **1988**, *60* (6), 514−516.
(35) Tsvirko, M. P.; Kalota, B.; Mikus, A.; Ostrowski, S. Structure and Luminescence Properties of Lutetium(Iii) Complexes with 5,10,15,20-Tetraphenylporphine and its Derivatives. *J. Appl. Spectrosc.* **2020**, *87* (5), 789−795.
(36) Van Uitert, L. G.; Soden, R. R. Emission Spectra of Trivalent Thulium. *J. Chem. Phys.* **1961**, *34* (1), 276−279.
(37) Kramer, R. *Chemometric Techniques for Quantitative Analysis*; CRC Press, 1998..
(38) Harris, D. C.; Lucy, C. A. *Quality Assurance and Calibration Methods. In Quantitative Chemical Analysis*, 9 ed.; Schultz, L., Ed.; W.H.Freeman& Company, 2016; p 105.
(39) Deng, B.; Wang, X.; Luong, D. X.; Carter, R. A.; Wang, Z.; Tomson, M. B.; Tour, J. M. Rare earth elements from waste. *Sci. Adv.* **2022**, *8* (6), No. eabm3132.
(40) Gergoric, M.; Ekberg, C.; Steenari, B.-M.; Retegan, T. Separation of Heavy Rare-Earth Elements from Light Rare-Earth Elements Via Solvent Extraction from a Neodymium Magnet Leachate and the Effects of Diluents. *J. Sustain. Metall.* **2017**, *3* (3), 601−610.
(41) Zhang, W.; Honaker, R. Q. Rare earth elements recovery using staged precipitation from a leachate generated from coarse coal refuse. *Int. J. Coal Geol.* **2018**, *195*, 189−199.
(42) Xiao, F.; Hu, W.; Zhao, J.; Zhu, H. Technologies of Recycling REEs and Iron from NdFeB Scrap. *Metals* **2023**, *13* (4), 779.
(43) *Critical Materials Assessment*; U.S. Department of Energy, 2023.
(44) Vaziri Hassas, B.; Shekarian, Y.; Rezaee, M. Selective precipitation of rare earth and critical elements from acid mine drainage - Part I: Kinetics and thermodynamics of staged precipitation process. *Resour. Conserv. Recycl.* **2023**, *188*, 106654.
(45) Sharp, E. J.; Weber, M. J.; Cleek, G. Energy Transfer and Fluorescence Quenching in Eu- and Nd-Doped Silicate Glasses. *J. Appl. Phys.* **1970**, *41* (1), 364−369.
(46) Holloway, W. W.; Kestigian, M. Quenching of the Tb3+ Fluorescence by Other Rare-Earth Ions in Aqueous Chloride Solutions. *J. Chem. Phys.* **1967**, *47* (5), 1826−1829.
(47) Kolar, E.; Catthoor, R. P. R.; Kriel, F. H.; Sedev, R.; Middlemas, S.; Klier, E.; Hatch, G.; Priest, C. Microfluidic solvent extraction of rare earth elements from a mixed oxide concentrate leach solution using Cyanex® 572. *Chem. Eng. Sci.* **2016**, *148*, 212−218.
(48) El Maangar, A.; Theisen, J.; Penisson, C.; Zemb, T.; Gabriel, J.-C. P. A microfluidic study of synergic liquid−liquid extraction of rare earth elements. *Phys. Chem. Chem. Phys.* **2020**, *22* (10), 5449−5462.

https://doi.org/10.1021/acssensors.5c00833
ACS Sens. XXXX, XXX, XXX−XXX